Molecular Crystals and Liquid Crystals
Publication details, including instructions for authors and subscription information:
http://www.tandfonline.com/loi/gmcl20

Comparison of Combustion and Solid-State Reaction Methods for the Fabrication of SOFC LSM Cathodes

Seon-Ho Yang [a], Kyung-Hwan Kim [a], Hyon-Hee Yoon [b], Woo-Jae Kim [b] & Hyung-Wook Choi [a]

[a] Department of Electrical Engineering, Kyungwon University, Korea

[b] Division of Energy and Biological Engineering, Kyungwon University, Korea

Version of record first published: 16 May 2011

To cite this article: Seon-Ho Yang, Kyung-Hwan Kim, Hyon-Hee Yoon, Woo-Jae Kim & Hyung-Wook Choi (2011): Comparison of Combustion and Solid-State Reaction Methods for the Fabrication of SOFC LSM Cathodes, Molecular Crystals and Liquid Crystals, 539:1, 50/[390]-57/[397]

To link to this article: http://dx.doi.org/10.1080/15421406.2011.566053

Mol. Cryst. Liq. Cryst., Vol. 539: pp. 50/[390]–57/[397], 2011

ISSN: 1542-1406 print/1563-5287 online
DOI: 10.1080/15421406.2011.566053

Taylor & Francis
Taylor & Francis Group

Comparison of Combustion and Solid-State Reaction Methods for the Fabrication of SOFC LSM Cathodes

SEON-HO YANG,[1] KYUNG-HWAN KIM,[1] HYON-HEE YOON,[2] WOO-JAE KIM,[2] AND HYUNG-WOOK CHOI[1]

[1]Department of Electrical Engineering, Kyungwon University, Korea
[2]Division of Energy and Biological Engineering, Kyungwon University, Korea

This study investigates the crystal phase and microstructure of LSM ($La_{1-x}Sr_xMnO_3$) cathode material synthesized by solid state reaction method and combustion synthesis. It measures and compares their electrical properties. LSM is a lanthanum ferrite-based cathode material. It has an ABO_3 perovskite structure; the A in this structure was substituted by Sr in this research to synthesize the LSM cathode powder. An electrolyte pellet was prepared using 8 mol% YSZ (yttria-stabilized zirconia) powder. The electrode was vapor deposited by screen printing. The crystal structure and morphology were measured by scanning electron microscopy (SEM) and X-ray diffraction (XRD) for the sintered samples collected. The complex impedance was measured in the temperature range 600–900°C in air (Computer Impedance Grain-Phase Analyzer). The electrical conductivity and polarization resistance of LSM were characterized systematically.

Keywords Cathode; LSM; SOFCs

Introduction

Solid oxide fuel cells (SOFCs), offering a low-pollution technology to generate electricity electrochemically with high efficiency, exhibit a great potential in solving the energy crisis and environment pollution [1]. Solid oxide fuel cells (SOFCs) with a high chemical to electrical energy conversion efficiency have been of a great interest for use as an alternative energy source. However, long-term stability, cost effective and large scale production and commercialization of thin film electrodes and electrolytes require reducing the operating temperature, whilst maintaining high electrocatalytic activity for the intermediate temperature SOFCs (IT-SOFCs). Material selection for cell construction is one approach considered to produce high performance viable IT-SOFCs. So far, it has all the electrode properties, such as high electrical conductivity and relatively high electrocatalytic activity for O2 reduction,

Address correspondence to Hyung-Wook Choi, Kyungwon University, San65 Bokjeong-dong, Sujeong-gu, Seongnam Gyunggi-do, Korea(ROK) 461-701. Tel.: (+82)31-750-5562; Fax: (+82)31-750-5491; E-mail: chw@kyungwon.ac.kr

and good thermal and chemical compatibility with yttria-stabilized zirconia (YSZ) electrolyte lanthanum strontium manganite (LSM), as a promising material for use in SOFCs [2–5]. $La_{1-x}Sr_xMnO_3$ perovskite (LSM) is regarded as one of the most promising cathode materials for solid oxide fuel cells (SOFCs) due to its high thermal and chemical stability and high electrocatalytic activity for oxygen reduction at high temperatures. These are the most extensively studied and investigated materials for O_2 reduction [6–9]. The sintering ability of LSM cathodes is found to be related to the strontium dopant level and stoichiometric composition of $(La,Sr)_xMnO_3$. It has been shown that LSM with an A-site deficient composition (x b1) sinters more readily than their B-site deficient counterparts (x N1) [10–11]. The synthesis of powder by the combustion method can produce a homogenous product in a short time without the use of expensive high-temperature furnaces. This synthesis technique makes use of the heat energy liberated by the exothermic redox reaction between metal nitrates and urea or other fuels at a relative low ignition temperature [12]. The cathode materials prepared using the conventional solid-state reaction were bigger, with an irregular morphology, unsuited to the desired application. The combustion process [13–15] used to prepare the phosphor is very facile, and only takes a few hours. In this paper, cathode materials were synthesized using a combustion method and solid-state reaction method. Thus, we investigate the crystal phase and microstructure of LSM ($La_{1-x}Sr_xMnO_3$) cathode material synthesized by a solid state reaction method and combustion synthesis. We measure and compare their electrical properties.

Experimental

1. *Preparation of the LSM Cathode*

Solid State Reaction Method. La_2O_3(99.99%, Aldrich), SrO (99.9%, Aldrich), MnO_2 (99.99%, Aldrich) were used as the starting materials to synthesize $La_{1-x}Sr_xMnO_3$ by the solid-state reaction method. The mixture of starting materials in the compositions $La_{1-x}Sr_xMnO_3$ ($x = 0.2$) was mixed sufficiently and ball-milled for 24 h (with IPA). After the mixture was heated at 80°C, this powder was calcined in air at 850°C for 4 h. This powder was cooled at a cooling rate of 5°C/min, ground, mixed again and ball-milled for 24 h (with IPA). After the mixture was heated at 80°C, it was sintered at 1000°C, 1200°C, 1300°C and 1400°C for 4 h.

Combustion Method. In this study, $La_{0.8}Sr_{0.2}MnO_3$ cathodes were prepared using the Combustion method. $La(NO_3)_3 \cdot 6H_2O$ (99.999%, Aldrich), $Sr(NO_3)_2$ (99.995%, Aldrich), $Mn(NO_3)_2 \cdot xH_2O$ (99.99%, Aldrich), Glycine A.C.S regent (98.5 + %, Aldrich) were used as starting materials. The nitrates ($La(NO_3)_3 \cdot 6H_2O$, $Sr(NO_3)_2$, $Mn(NO_3)_2 \cdot XH_2O$) were dissolved in de-ionized water at 80°C. Glycine as a fuel served as the oxidizer. The Glycine solution was heated to 80°C and continuously stirred using a magnetic bar. The nitrate solution was dropped into the fuel, and was continued to be heated for 30 min at 80°C. The solution was then transferred to a pre-heated furnace at 300°C. Then, the pre-heated samples were sintered in the furnace for 4 hours at 800∼1400°C.

2. *Preparation of the Half Cell*

Electrolyte pellets were prepared from a 8%mol YSZ (YSZ8-TC) commercial powder provided by Fuel Cell Materials (FCM). Cylindrical pellets 0.099 ± 0.001 cm

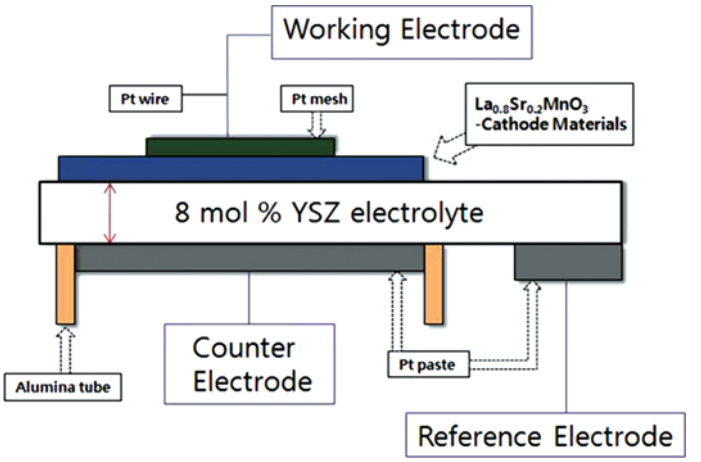

Figure 1. Schematic diagram of half-cell.

thick and 1.39 ± 0.01 cm in diameter were formed after uniaxial pressing and sintering at 1600°C for 4 h in air. The resultant LSM powders were then mixed with a vehicle to form a paste applied to a YSZ pellet by screen printing. The pellets were then sintered at 1200°C and used as the working electrode. Figure 1 is a schematic of the half-cell configuration. The Pt counter and reference electrodes were deposited on the reverse side of the YSZ, and the entire cathode sintered at 1000°C for 3 h.

Measurements

The crystalline development of the resulting samples was checked by X-ray diffraction (XRD, model D/MAX-2200) using CuKα-radiation in the range of $2\theta = 20 \sim 80$°C. The morphology and the size of the prepared particles were investigated with a field-emission scanning electron microscope (FE-SEM, model S-4700, HITACHI). The complex impedance was measured in the temperature range 600–900°C in air (Cell tester, Probo stat, NorECS).

Results and Discussion

Figures 2 and 3 show the XRD patterns of the $La_{0.8}Sr_{0.2}MnO_3$ cathode powders formed by the solid-state and combustion methods. The patterns indicate the crystalline structure produced for the LSM powders at the different sintering temperatures. Figure 2 shows the XRD-patterns of the LSM powder sintered at 800~1400°C by the combustion method. 1000°C, 1200°C and 1400°C patterns showed a perovskite crystalline structure. The patterns indicated the intensity of the perovskite phase was shown to increase with the sintering temperate. However, at 800°C the XRD pattern is not a perovskite crystalline structure. Therefore, the LSM in the synthesis is satisfactory at a sintering temperature above 1000°C. However, impurities peaks were observed due to the quenching effect of high temperature at 1400°C. Figure 3 shows XRD-patterns of the LSM powder sintered at 1000~1400°C by the solid-state reaction method. For LSM powder sintered at 1000°C both the perovskite phase, and the La_2O_3 peaks due to not having synthesized, were

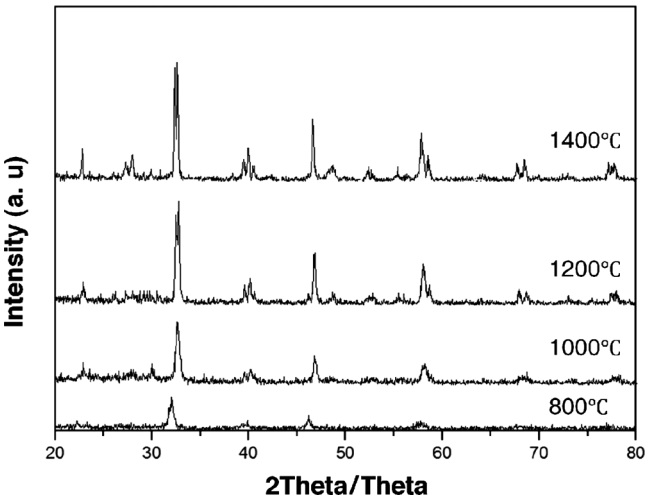

Figure 2. XRD pattern of LSM cathode powders by combustion method.

observed. Sintering at 1200°C resulted in a perovskite crystalline structure, but sintering at 1300°C and 1400°C did not result in a perovskite crystalline structure. In both of these methods the exact XRD-patterns of the perovskite crystalline structure could be observed when the sintering temperature was at 1200°C. The composite materials are considered to be satisfactory when a sintering process at 1200°C for 4 h is used.

Figures 4 and 5 shows the SEM images of LSM powder sintered at different temperatures by the combustion method and solid-state reaction method. Figure 4 shows that the cathode particle sizes become larger with increasing temperature. However, agglomerates formed particles due to the high sintering temperature at

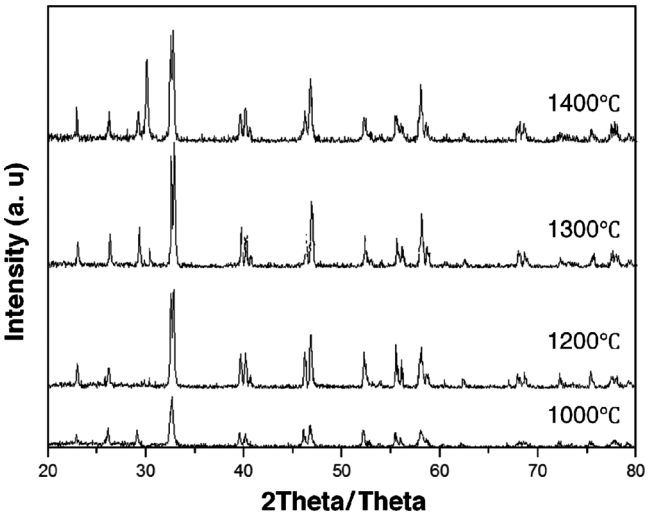

Figure 3. XRD pattern of LSM cathode powders by solid-state reaction method.

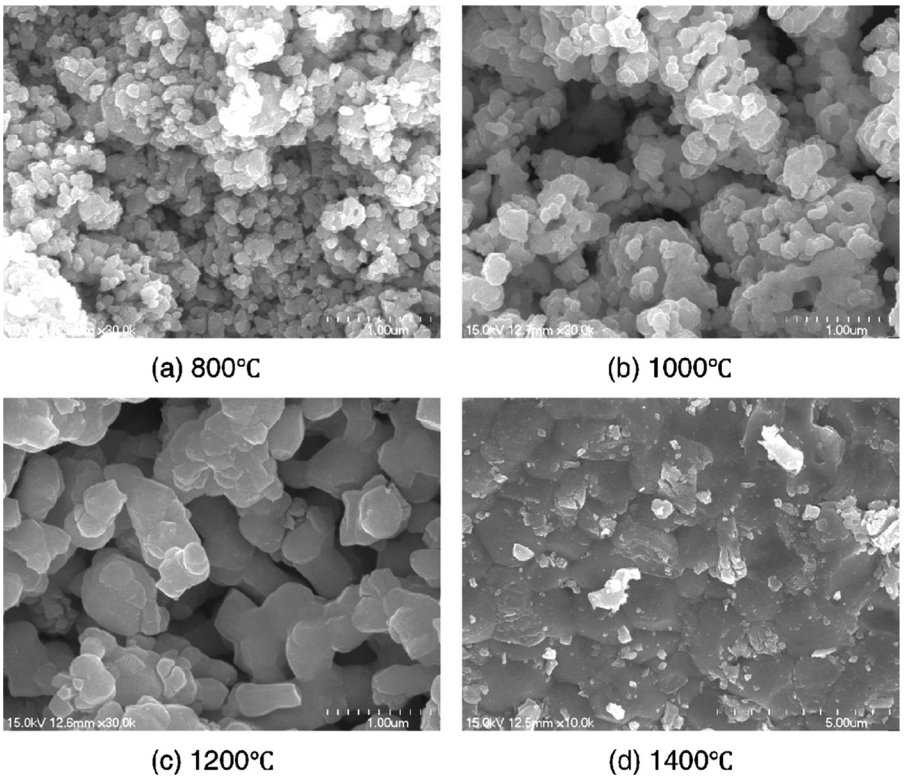

Figure 4. FESEM image of LSM cathode powders by combustion method.

1400°C. At this point, we estimated that the characteristics of the powders had been improved by increasing the sintering temperature; Figure 4(d) shows the microstructure of the melted particle. The cathode particle sizes in Figure 5(b) are smaller than those in Figure 5(c), (d) and the porosity of the cathode in Figure 5(b) seems lager than that in Figure 5(c), (d). With an increased sintering temperature, particle size has grown. However, defects form in the LSM powder when it is heated beyond a critical temperature.

Sintering the composite materials at 1200°C for 4 h is considered satisfactory, as impedance diagrams were plotted 1173 K, during both the heating and cooling cycles to measure the conductivity changes after annealing by sintered at 1200°C for LSM powder. Table 1 shows polarization resistance for different operating temperatures. Table 1 shows decreased polarization resistance with increasing operating temperature. The electrode kinetics is very active at high temperatures due to the increased operating temperature. The cathode electrode by combustion method has smaller polarization resistance than the solid-state reaction method. The increase in resistance is considered due to the formation of minute impurities peaks (XRD-patterns). Figure 6 shows electrical conductivity of LSM for various operating temperatures (873 K$\sim$1173 K). The electrical conductivity was obtained from the following equation.

$$R = \rho \frac{1}{A} \tag{1}$$

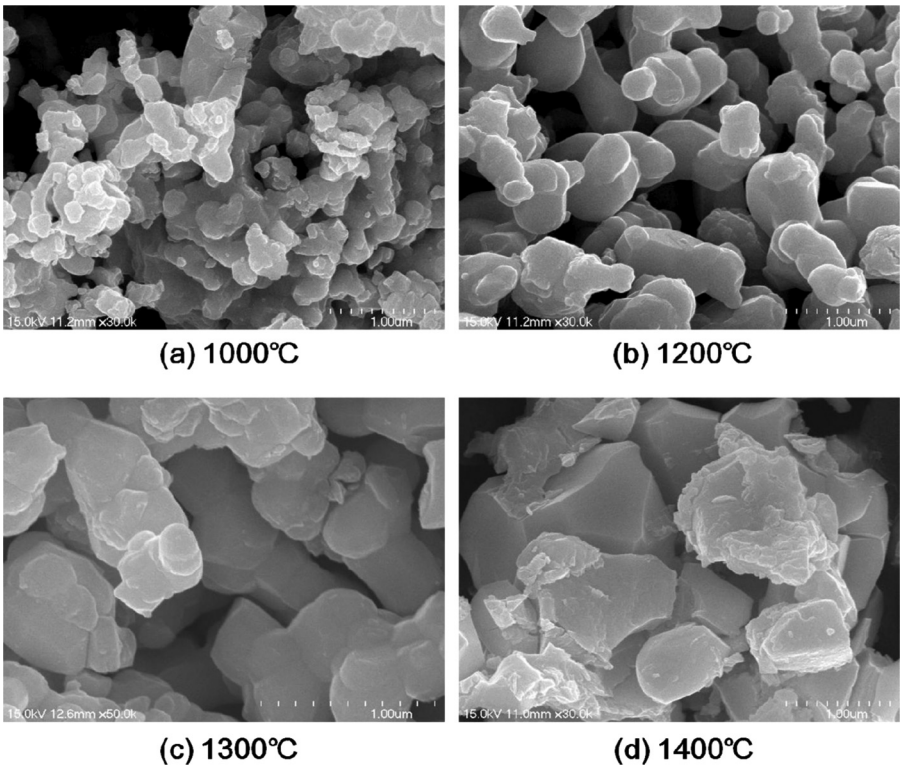

Figure 5. FESEM image of LSM cathode powders by solid-state reaction method.

(R = Polarization Resistance, A = the area of the cathode, l = the thickness of the cathode, ρ = Specific resistance).

Electrical conductivity values were obtained through the inverse of the specific resistance. Figure 6 shows the increased electrical conductivity by increasing the operating temperature.

This work indicates the LSM cathode prepared by combustion method has higher polarization resistance and smaller electrical conductivity than that formed in the solid-state reaction method.

Table 1. Polarization resistance of LSM cathode materials

	LSM by Solid-state method	LSM by combustion method
Operating temperature	Polarization resistance (Ω cm^2)	Polarization resistance (Ω cm^2)
873 K	83.37	72.54
973 K	31.43	27.64
1073 K	13.05	12.64
1173 K	11.76	10.82

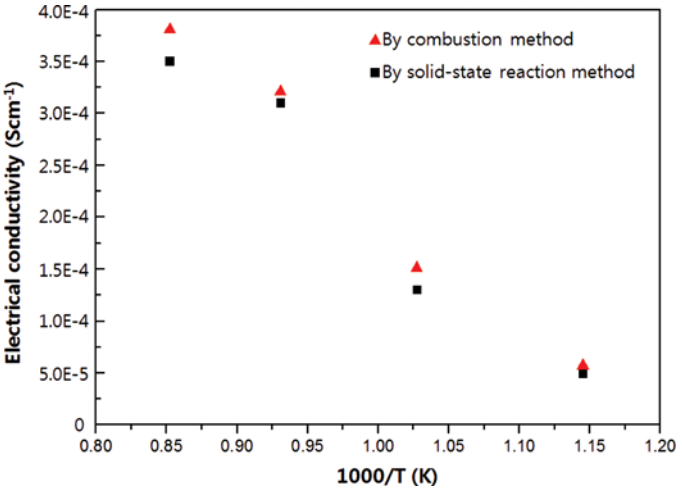

Figure 6. Arrhenius plots of the electrical conductivity of LSM for various operating temperature.

Conclusions

This study compares the Combustion and Solid-State reaction methods for fabrication of SOFC LSM cathodes. The exact XRD-patterns of the perovskite crystalline structure when the sintering temperature was at 1200°C could be observed in both methods. The composite material is considered satisfactory in a sintering process at 1200°C for 4 h. Particle size grows with increased sintering temperature. However, defects form in the LSM powder when it is heated beyond a critical temperature above 1300°C. Therefore, LSM cathodes were considered satisfactory in a sintering process at 1200°C. Impedance diagrams were plotted 1173 K, during both the heating and cooling cycles to measure the conductivity changes after annealing. The samples synthesized at 1200°C by combustion method had the smallest polarization resistance 10.82 (Ω cm^2) and relatively good performance when the operating temperature is 1173 K. In addition, the samples formed by the combustion method had the highest electrical conductivity 3.8E-4 (Scm^{-1}). Although there was not a large difference between the two methods, the combustion method had better electrical characteristics than the solid-state reaction method. The combustion method is anticipated to be very attractive for low cost synthesis, as it is a simple process and saves time.

Acknowledgment

This work was supported by the Human Resources Development of the Korea Institute of Energy Technology Evaluation and Planning (KETEP) grant funded by the Korea government Ministry of Knowledge Economy (*No. 20104010100510*).

References

[1] Singhal, S. C. (2002). *Solid State Ion.*, *405*, 152–153.
[2] Li, J. Q., & Xiao, P. (2001). *Eur. J. Ceram. Soc.*, *21*, 659–668.

[3] Wang, W., & Jiang, S. P. (2006). *Solid State Ionics*, *177*, 1361–1369.
[4] Wang, H. B., Meng, G. Y., & Peng, D. K. (2000). *Thin Solid Films*, *368*, 275–278.
[5] Grundy, A. N., Hallstedt, B., & Gauckler, L. J. (2004). *CALPHAD*, *28*, 191–201.
[6] Minh, N. Q. (1993). *J. Am. Ceram. Soc.*, *76*(3), 563–588.
[7] Zheng, F., & Pederson, L. R. (1999). *J. Electrochem. Soc.*, *146*, 2810.
[8] Decorse, P., Caboche, G., & Dufour, L.-C. (1999). *Solid State Ionics*, *117*, 161.
[9] Islam, M. S., Cherry, M., & Winch, L. J. (1996). *J. Chem. Soc., Faraday Trans.*, *92*, 479.
[10] Simwonis, D., Tietz, F., & Stfver, D. (2000). *Solid State Ionics*, *132*, 241.
[11] Jiang, S. P. (2003). *Mater. J. Sci.*, *38*, 3775.
[12] Yin, S. Y., Chen, D. H., & Tang, W. J. (2007). *J. Alloys Compd.*, *441*, 327–331.
[13] Xu, L., Wei, B., Zhang, Z., Lu, Z., Gao, H., & Zhang, Y. (2006). *Nanotechnology*, *17*, 4327.
[14] Zhang, J., Ning, J., Liu, X., Pan, Y., & Huang, L. (2003). *Mater. Res. Bull.*, *38*, 1249–1256.
[15] Bang, J., Abboudi, M., Abrams, B., & Holloway, P. H. (2004). *J. Lumin.*, *106*, 177–185.